Naval Research Laboratory

Washington, DC 20375-5320

NRL/MR/6111--15-9663

The Effect of Substrate Emissivity on the Spectral Emission of a Hot-Gas Overlayer

HAROLD D. LADOUCEUR
JOHN D. KIRTLEY
SYED N. QADRI
JEFFREY C. OWRUTSKY

Chemical Dynamics and Diagnostics Branch
Chemistry Division

DANIEL A. STEINHURST

Nova Research, Inc.
Alexandria, Virginia

December 30, 2015

REPORT DOCUMENTATION PAGE

Form Approved
OMB No. 0704-0188

1. REPORT DATE *(DD-MM-YYYY)*	**2. REPORT TYPE**	**3. DATES COVERED** *(From - To)*
30-12-2015	Memorandum	January – August 2015

4. TITLE AND SUBTITLE

The Effect of Substrate Emissivity on the Spectral Emission of a Hot-Gas Overlayer

5a. CONTRACT NUMBER

5b. GRANT NUMBER

5c. PROGRAM ELEMENT NUMBER

6. AUTHOR(S)

Harold D. Ladouceur, John D. Kirtley, Syed N. Qadri,
Jeffrey C. Owrutsky, and Daniel A. Steinhurst[1]

5d. PROJECT NUMBER

5e. TASK NUMBER

5f. WORK UNIT NUMBER

7. PERFORMING ORGANIZATION NAME(S) AND ADDRESS(ES)

Naval Research Laboratory
Code 6111
4555 Overlook Avenue, SW
Washington, DC 20375-5344

8. PERFORMING ORGANIZATION REPORT NUMBER

NRL/MR/6111--15-9663

9. SPONSORING / MONITORING AGENCY NAME(S) AND ADDRESS(ES)

Office of Naval Research
One Liberty Center
875 North Randolph Street, Suite 1425
Arlington, VA 22203-1995

10. SPONSOR / MONITOR'S ACRONYM(S)

ONR

11. SPONSOR / MONITOR'S REPORT NUMBER(S)

12. DISTRIBUTION / AVAILABILITY STATEMENT

Approved for public release; distribution is unlimited.

13. SUPPLEMENTARY NOTES

[1]Nova Research, Inc., 1900 Elkin Street, Suite 230, Alexandria, VA 22906

14. ABSTRACT

Fourier transform infrared (FTIR) emission spectroscopy, recently implemented for *in operando* testing of solid oxide fuel cell (SOFC) anodes by Pomfret and coworkers, has become a novel means to directly measure the radiative emission of hot gases within the volume over an anode surface. Ideally, the FTIR detector will only see the infrared emission of the hot anode surface and any gases in the anode head space, though in reality broad-band, non-molecular (and frequency-dependent) emission sources (e.g., furnace walls) can contribute to the signal reaching the detector via geometric form factors. These contributions must be removed from each spectrum collected during an experiment to leave behind the difference that shows only molecular contributions. This report describes the effect of background surface emissivity on the gas emission spectrum. An analytic model, which is confirmed by numerical analysis, is developed and demonstrates that the emitted background radiation is indeed coupled to gas-phase molecular emissions in a nonlinear way and cannot be completely removed from the molecular gas spectrum by subtraction of the background spectrum.

15. SUBJECT TERMS

Radiative transfer
Solid oxide fuel cell (SOFC)
Spectral emission
FTIR emission spectroscopy
Form factor
Configuration factor

16. SECURITY CLASSIFICATION OF:			**17. LIMITATION OF ABSTRACT**	**18. NUMBER OF PAGES**	**19a. NAME OF RESPONSIBLE PERSON**
a. REPORT	**b. ABSTRACT**	**c. THIS PAGE**			Harold D. Ladouceur
Unclassified Unlimited	Unclassified Unlimited	Unclassified Unlimited	Unclassified Unlimited	19	**19b. TELEPHONE NUMBER** *(include area code)* (202) 767-3558

Standard Form 298 (Rev. 8-98)
Prescribed by ANSI Std. Z39.18

CONTENTS

EXECUTIVE SUMMARY

Fourier transform infrared emission spectroscopy was recently implemented for *in operando* studies of high temperature solid oxide fuel cells (SOFCs). The method is intended to detect and spectrally resolve selective emission from molecular species on or above the anode, i.e. for hot gases over the anode. However, the substrate and other broad-band emission sources (e.g. furnace walls) contribute to the signals observed and complicate their analysis and interpretation. These effects must be accounted for in order to estimate the sensitivity to selective emission and to segregate the molecular components of the emission. This report describes the effects of background surface emissivity on the observed spectral radiant intensity from a hot gas located above the background surface. An analytic model is developed and confirmed numerically. It demonstrates that the emitted background radiation is coupled to gas-phase molecular emissions in a nonlinear way and cannot be completely removed from the molecular gas spectrum by direct subtraction of the background spectrum. The emission spectrum also depends upon the experimental geometry through the radiative form factors.

The Effect of Substrate Emissivity on the Spectral Emission from a Hot-Gas Overlayer

INTRODUCTION

Recently, *in operando* optical investigations of high temperature solid oxide electrochemical cells (SOECs) have gained significant traction with several research groups [1-8] motivated by a need to directly correlate electrochemical performances of SOECs with their associated and complex electrode processes. These techniques (including Raman spectroscopy, ambient x-ray photoelectron spectroscopy, near-infrared thermal imaging, and Fourier transform infrared emission spectroscopy) have demonstrated a significant advantage over traditional, indirect experimental methods by providing direct, non-invasive information in real time along with high temporal, spatial, and/or molecular resolution. Fourier transform infrared emission spectroscopy, recently implemented for *in operando* testing of solid oxide fuel cell (SOFC) anodes by Pomfret and coworkers, [4] has become a novel means to directly measure the radiative emission of hot gases within the volume over an anode surface, including CH_4, CO_2, CO, and H_2O (see Figure 1). In these measurements, a FTIR spectrometer was adapted by removing an infrared glow source from the optical path and aligning in its place the anode surface, located within a furnace cavity. Ideally, the detector will only see the infrared emission of the hot anode surface and any gases in the anode head space, though in reality broad-band, non-molecular (and frequency dependent) emission sources (e.g. furnace walls) contribute to the majority of the signal reaching the detector. These must be subtracted from each spectrum collected during an experiment to leave behind the difference that shows only molecular contributions.

However, recent emission experiments have indicated that for the FTIR spectra a simple background subtraction may not account for all background contributions. These measurements have been made on a variety of fuels including 100% CH_4 and mixtures of CH_4/Ar and simulated biogas (50% CH_4 and 50% CO_2, balance Ar) at various operational temperatures which represent different SOFC operating conditions. *In operando* IR emission spectra collected during operation with both fuels described above show that CO_2 emission is significantly attenuated relative to other gas constituents (Figure 2). On the other hand, *ex situ* IR absorption measurements from the same experiments have demonstrated that CO_2 absorption is optically thick and very intense relative to other gas constituents in the spectrum. Additionally, attempts to calibrate the emission intensity of CO_2 with concentration in a high-temperature environment indicated a nonlinear response, while FT-IR absorption measurements of the same gases directed into a flow cell showed a linear response as expected. Interestingly, in the emission experiments, as the concentration of CO_2 increased, the normally weak CO_2 combination bands at 3600 cm^{-1} and 3700 cm^{-1} grew in intensity while the asymmetric stretch at 2350 cm^{-1} remained relatively unchanged. We expect that the gas composition over the anode headspace is comparable to the exhaust composition, despite the rather large apparent concentration differences inferred from the emission and absorption spectra. To better understand these differences, a model has been implemented to describe how the frequency-dependent substrate emission could affect the emission of a hot gas. This report describes a model where the background radiation is coupled to molecular emission, and cannot be subtracted

Manuscript approved November 24, 2015

linearly. Furthermore, the geometry of the test apparatus greatly influences any background radiation through the radiative form factor and reflections from the anode surface.

A similar analysis had been developed previously to describe the conditions necessary for selective emission from a heated solid coating on a substrate. In an earlier NRL memorandum report, [9] this problem was investigated using an analytic two-flux radiation model. There it was demonstrated that in order to have selective emission from the coating, the emissivity of the substrate must be less than the emissivity of the coating. In Figure 3, taken from reference 9, the calculated spectral emission of a 110 mil thick coating of SiO_2 on steel shows selective emission since $\varepsilon_{SiO2} > \varepsilon_{steel}$. The calculation assumed that substrate and the SiO_2 coating were at the same temperature (1273 K).

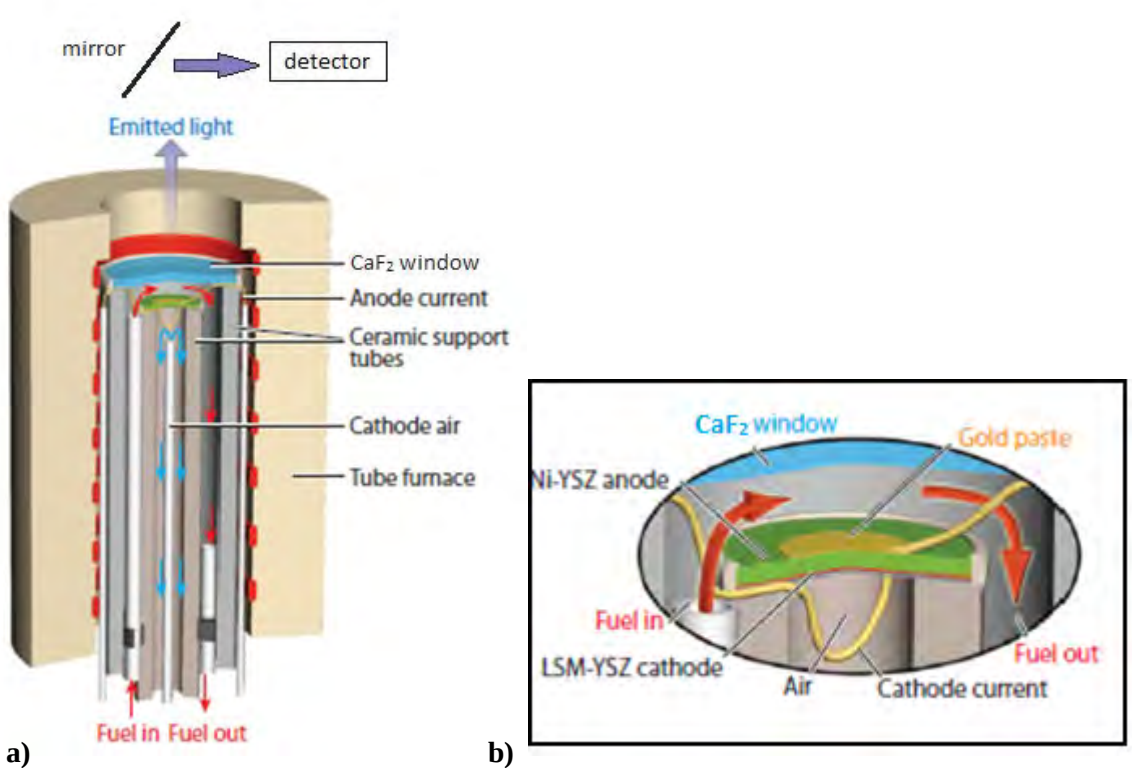

Figure 1. A schematic of the Fourier Transform Infrared Emission SOFC test assembly is shown on the left (a). A more detailed view of the headspace between the anode and the CaF_2 window can be seen in (b). Modified from original figure by R. J. Kee.

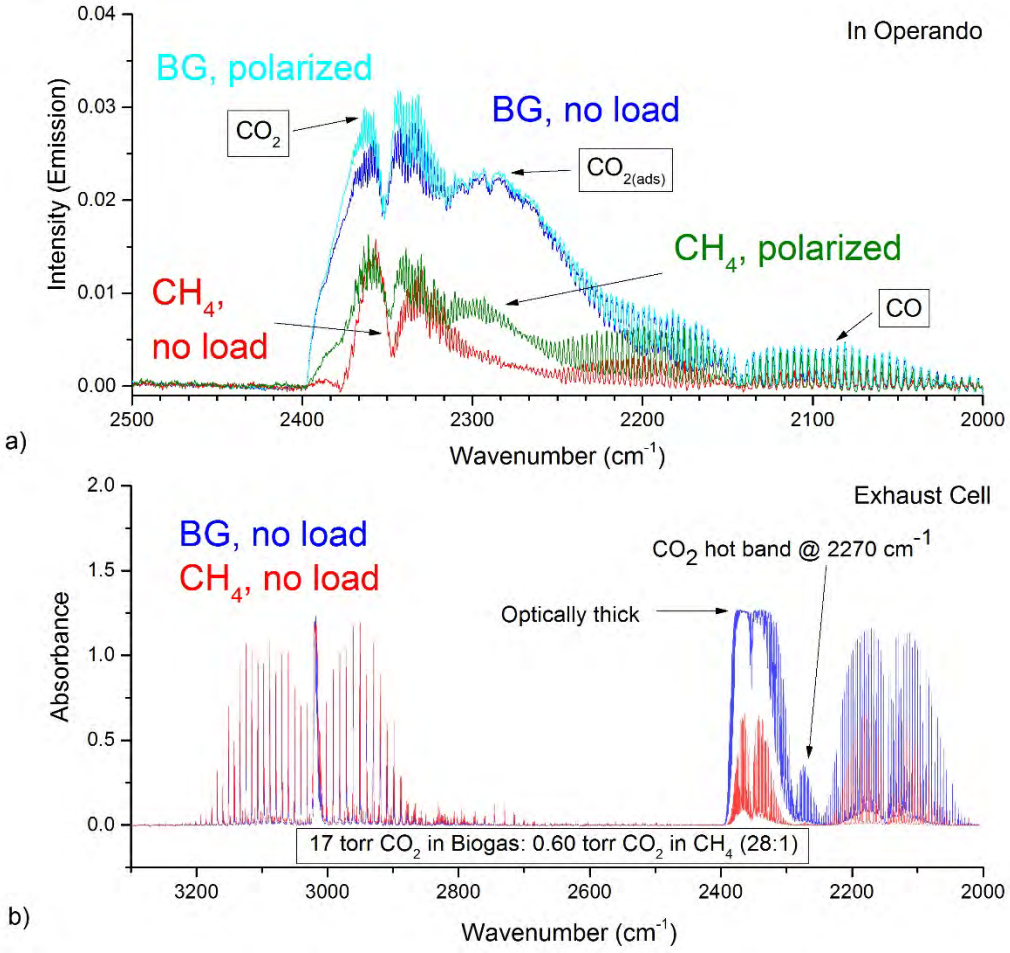

Figure 2. FTIR emission spectra collected from a Ni/YSZ anode-supported SOFC operating with simulated biogas (BG), CH_4, CO and CO_2 at 800 °C are shown in (a) and corrected with a linear baseline subtraction. Optical path length was approximately 5 mm. During the same trial, anode exhaust was fed into a 10 cm gas cell and the absorbance was measured with an FTIR spectrometer (b).

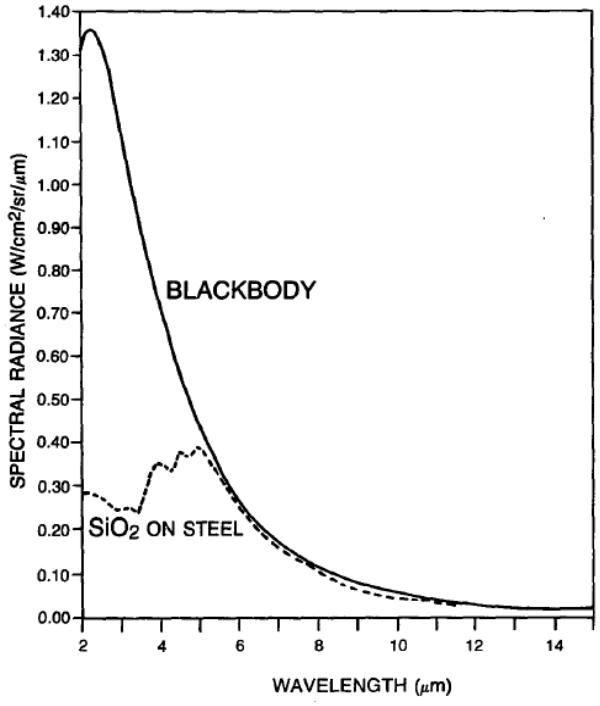

Figure 3. Selective emission from SiO_2 coating over steel substrate at 1273 K. Coating is 110 mils thick.

RADIATIVE TRANSFER EQUATION

The background contributions observed in an emission experiment could arise from the hot walls of a furnace via reflection or a hot surface oriented normal to the direction of observation through the emitting gas, e.g. an anode in an active solid oxide fuel cell. The hot emitting gas is assumed to be at a spatially uniform given temperature T. The radiative contributions of the furnace walls and other surfaces within the observation region are introduced as boundary conditions imposed on the radiative transfer equation[10]

$$\frac{\mathrm{dI}(\lambda,\mathrm{T})}{\mathrm{ds}} = \kappa(\lambda)\mathrm{I}(\lambda,\mathrm{T})_{\mathrm{BB}} - \kappa(\lambda)\mathrm{I}(\lambda,\mathrm{T}) - \sigma_{\mathrm{sc}}\mathrm{I}(\lambda,\mathrm{T}) + \frac{\sigma_{\mathrm{sc}}}{4\pi}\int \mathrm{I}(\lambda,\mathrm{T})\Phi\left(\lambda,\hat{\mathrm{S}}_{\mathrm{i}},\hat{\mathrm{S}}\right)\mathrm{d}\Omega,$$

where $\mathrm{I}(\lambda,\mathrm{T})$ denotes the spectral radiant intensity (radiative energy flow/time/area normal to rays/solid angle/wavelength), $\kappa(\lambda)$ denotes the spectral absorption coefficient, $\mathrm{I}(\lambda,\mathrm{T})_{\mathrm{BB}}$ is the blackbody Planck function, σ_{sc} is the linear scattering coefficient and $\Phi\left(\lambda,\hat{\mathrm{S}}_{\mathrm{i}},\hat{\mathrm{S}}\right)$ is a phase function associated with inward scattering of radiation from surrounding control volumes into the direction of observation about the differential solid angle $d\Omega$. This term increases the radiant intensity along the line of sight. The first term on the right-hand side corresponds to spectral emission from the gas, the second term represents spectral absorption by the gas and the third term accounts for scattering losses along the observation path s. The scattering processes are quite small in the absence of particulates (Mie scattering); therefore the last two

terms will be neglected in this analysis. Assuming the hot emitting surface is located at $s = 0$, the formal solution to the radiative transfer equation can be written as

$$I(\lambda, T, s) = I(0, \lambda, T_s)\exp(-\kappa(\lambda)s) + I(\lambda, T)_{BB}[1 - \exp(-\kappa(\lambda)s)].$$

The factor $I(0, \lambda, T_s)$ denotes the spectral intensity from the substrate located at s = 0. The transmittance of the gas $\tau(\lambda, s)$ over a distance s is defined from the Beer-Lambert law

$$\tau(\lambda, s) = \frac{I(s)}{I_0} = \exp(-\kappa(\lambda)s).$$

The absorbance A is defined as $A = -\log(\tau(\lambda, s))$. In the absence of scattering or reflections, the gas absorptivity or absorptance $\alpha(\lambda, s)$ is given by

$$\alpha(\lambda, s) = 1 - \tau(\lambda, s) = \varepsilon(\lambda, s).$$

By Kirchhoff's law, the gas emissivity $\varepsilon(\lambda, s)$ is equated to the absorptivity. Using these relations, we see that the observed spectral line intensity $I(\lambda, s)$ will be a combination of both the transmitted intensity from the surface and the emitted intensity from the gas

$$I(\lambda, s) = I(0, \lambda, T_s)\exp(-\kappa(\lambda)s) + I(\lambda, T_g)_{BB}[\varepsilon(\lambda, s)],$$

where allowance has been made for the substrate temperature T_s to be different from the gas temperature T_g.

The quantity $I(0, \lambda, T_s)$ represents the radiant spectral intensity from the surface at a given temperature T_s and in a particular direction. The calculated spectral intensity depends upon what assumptions are made about the substrate surface emissivity. The simplest case is to assume that the surface is a blackbody with $\varepsilon = 1$ and $T_s = T_g$. Under these assumptions, the observed spectral intensity from the substrate and gas overlayer is that of a blackbody at the common temperature T

$$I(\lambda, T, s) = I(\lambda, T)_{BB}\exp(-\kappa(\lambda)s) + I(\lambda, T)_{BB}[1 - \exp(-\kappa(\lambda)s)] = I(\lambda, T)_{BB} .$$

In the second case let the surface emissivity be that of a grey body with $0 < \varepsilon_s(\lambda) < 1$ and assume that there is no incident radiation upon the surface from the surroundings. The spectral intensity is given by

$$I(\lambda, s) = \varepsilon_s(\lambda)I(\lambda, T_g)_{BB}\exp(-\kappa(\lambda)s) + I(\lambda, T_g)_{BB}[\varepsilon(\lambda, s)].$$

This equation can be reduced to a more insightful form

$$I(\lambda, s) = \varepsilon_s(\lambda)I(\lambda, T_g)_{BB}(1 - \varepsilon(\lambda, s)) + I(\lambda, T_g)_{BB}[\varepsilon(\lambda, s)]$$

$$= (\varepsilon_s(\lambda) + \varepsilon(\lambda, s) - \varepsilon_s(\lambda)\varepsilon(\lambda, s))I(\lambda, T_g)_{BB}.$$

This result shows that simple linear subtraction of the substrate background from the spectrum does not completely remove the background due to the cross-term $\varepsilon_s(\lambda)\varepsilon(\lambda, s)$. Upon linear subtraction of the background contribution, the spectral intensity is given by

$$I(\lambda, T_g) = \varepsilon(\lambda, T_g) I(\lambda, T_g)_{BB} [1 - \varepsilon_s(\lambda)].$$

Note that the "corrected" spectral intensity is given as the product of two factors. The first factor $\varepsilon(\lambda, T_g) I(\lambda, T_g)_{BB}$ corresponds to the *molecular emission* or *absorption* (Kirchhoff's law) due to the gas in the absence of a substrate. The second factor, which is due to the substrate, reduces the spectral emission intensity.

MODEL CALCULATIONS

Figure 4 shows an idealized emission experiment. A nickel substrate is placed in a furnace at 1073 K and a layer of 10% by volume CO_2 is located above the substrate. Using the HITRAN[11] data base and a commercial code for calculating molecular spectra, [12] we will investigate the validity of the above formulae.

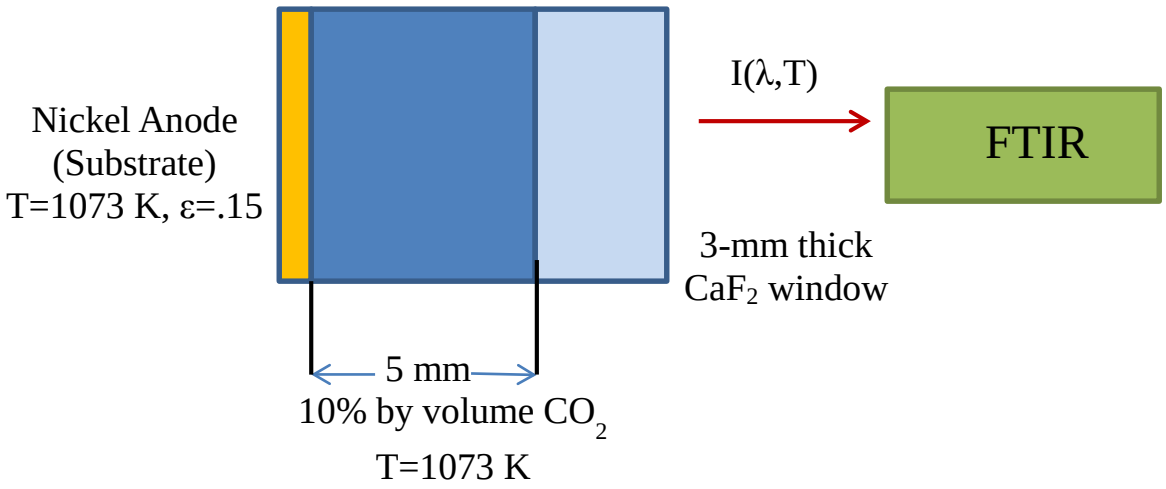

Figure 4. Geometry for idealized emission model.

For computational purposes, we will consider the CO_2 antisymmetric stretch ν_3 centered at 2349 cm^{-1} (4.26 μm). We will first calculate the spectral radiance ($W/m^2/sr/cm^{-1}$) emitted by the gas between 2200 cm^{-1} and 2400 cm^{-1} in the absence of a substrate utilizing the HITRAN line parameters and the Spectral Calculator code. The results of this calculation are shown in Figure 5.

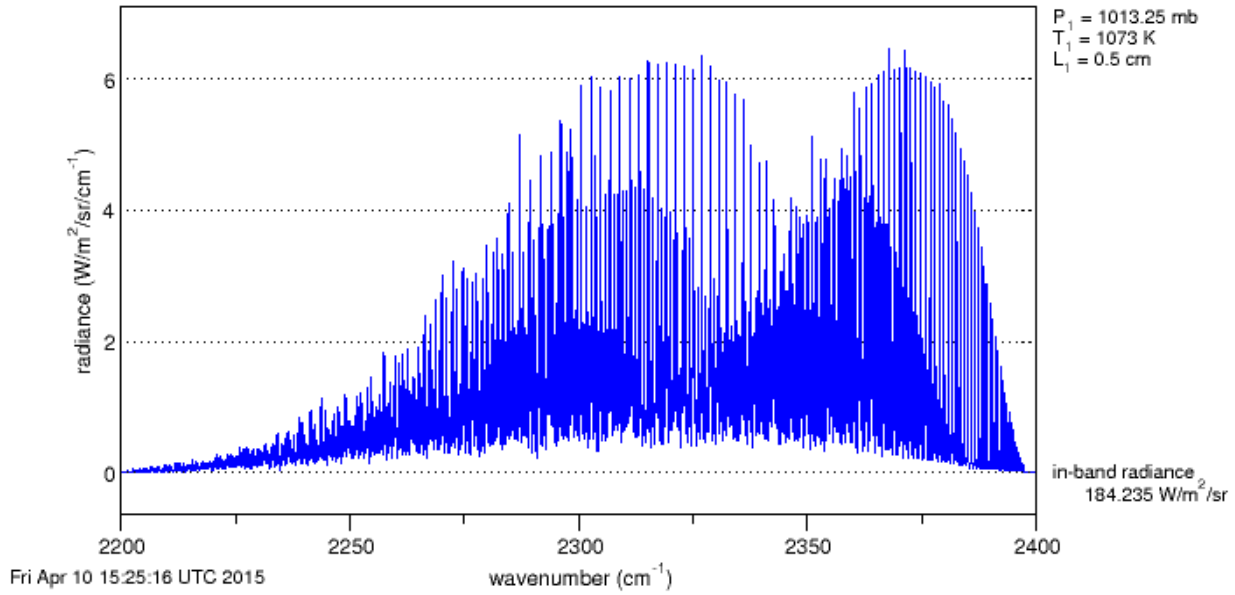

Figure 5. Calculated CO_2 spectral radiance without substrate.

The calculated in-band radiance (2200-2400 cm^{-1}) is 184.2 $W/m^2/sr$. Note that the baseline goes to zero in the wings. Using the same code, the blackbody in-band radiance is 1389.2 $W/m^2/sr$ as shown in Figure 6. Therefore, the carbon dioxide emissivity in this band at 1073 K is given by

$$\varepsilon_{CO2} = \frac{184.2}{1389} = 0.1326$$

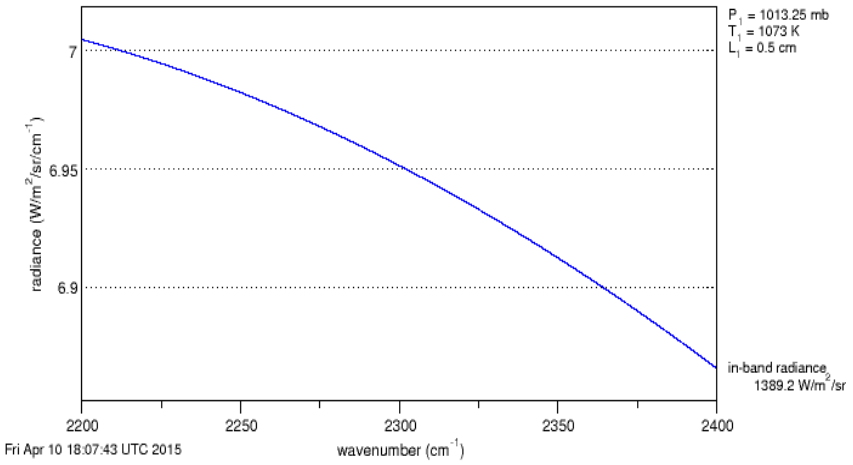

Figure 6. Calculated in-band Planck radiance.

We will now consider the effect of the anode surface on the spectral radiance. The anode is assumed to be made of nickel with an emissivity[13] $\varepsilon_s = 0.15$. The calculated spectral radiance is shown in Figure 7.

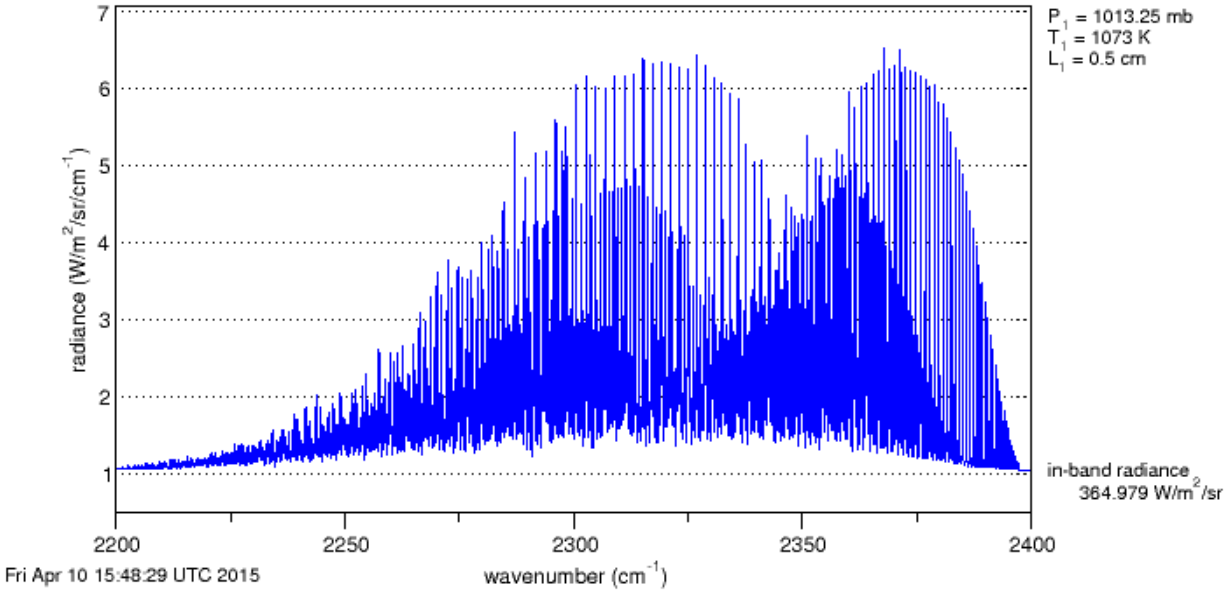

Figure 7. Calculated CO_2 spectral radiance with hot nickel substrate.

The calculated in-band radiance is 365.0 W/m^2/sr. The effective emissivity ε_{eff} of the anode-gas composite system based upon the in-band radiance is given by

$$\varepsilon_{eff} = \frac{365}{1389.2} = 0.263$$

The effective emissivity calculated from the analytic expression ($\varepsilon_s + \varepsilon(\lambda, s)$-$\varepsilon_s\, \varepsilon(\lambda, s)$) equals 0.263 which demonstrates the validity of the analytic model result. Note that the baseline does not go to zero in the wings due to the substrate emission.

If the substrate temperature T_s were higher than the gas temperature T_g, the observed spectral radiance would show an absorption feature at 2349 cm^{-1}. If the transmittance $\tau(\lambda, s)$ were zero in the 2349 cm^{-1} band and $T_s \neq T_g$, the observed band spectrum would be that of a blackbody at temperature T_g. If the gas temperature exceeded the surface temperature, the absorption lines would be inverted, becoming emission lines above the cooler blackbody substrate.

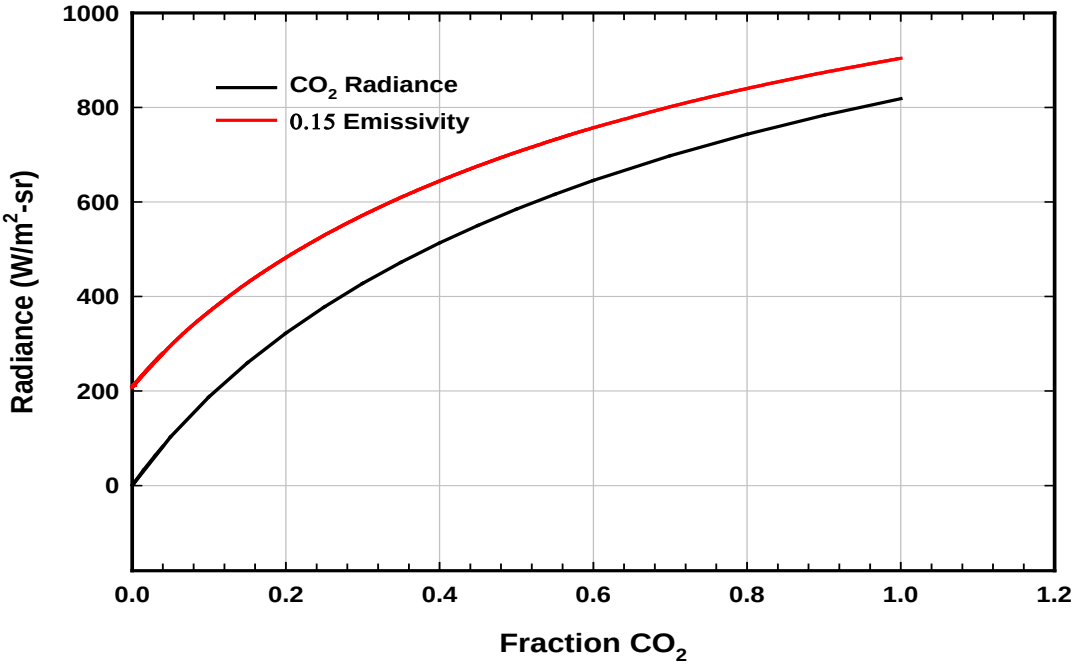

Figure 8. Calculated in-band (2200-2400 cm^{-1}) radiance as a function of CO_2 volume fraction. The black curve corresponds to CO_2 emission without a substrate. The red curve includes a background substrate with an emissivity ε=0.15. The gas temperature is 800°C and the path length is 5 mm.

Figure 8 shows a plot of the calculated in-band (2200-2400 cm^{-1}) radiances at 800°C as a function of CO_2 volume fraction (f). The black curve was calculated using the Spectral Calculator code over a 5 mm path length with a total pressure of 1 atm. The red curve repeated the calculation but included a substrate of emissivity 0.15 at 800°C. Both plots show a linear dependence upon concentration for small volume fractions of CO_2 ($f < 0.1$). As the CO_2 volume fraction increases, the emission spectra show a distinct curvature. This behavior is consistent with the Ladenburg-Reiche function for the curve of growth.[10] At low concentrations the behavior is linear. At higher concentrations the asymptotic behavior follows a square root function. The curve of growth is dependent upon the line strength, the concentration, the path length and the temperature.

EFFECTS OF SURROUNDING SURFACES

The gas emission model describe above is a one-dimensional spatial model for radiative transport. The radiation sources in this model are assumed to arise solely from spectral emission of the substrate (anode) and the overlayer of gas. In reality, the entire system would be embedded in a furnace with radiating walls and windows. The spectral emission from these surfaces can contribute to the observed radiance by spectral reflection from the substrate surface. The radiation incident upon the anode surface

arrives from all directions and is termed the spectral irradiation. The spectral irradiation is denoted by G_λ is given by

$$G_\lambda = \int_0^{2\pi} \int_0^{\pi/2} I(\lambda, T, \theta, \phi) \cos\theta \sin\theta d\theta d\phi$$

If the irradiation comes from *diffuse* surfaces, $I(\lambda, T, \theta, \phi)$ is independent of θ and φ and the irradiation is given by

$$G(\lambda)_i = \pi I_i(\lambda, T)$$

where the subscript denotes the i-th enclosure surface. The effects of reflection can be included in the analysis by modifying the boundary condition for $I(0, \lambda, T_s)$ at the anode surface location $s = 0$.

The spectral radiosity, denoted by $J_s(0, \lambda, T_s, T_{surf})$ accounts for both the emitted spectral energy and the reflected spectral energy from the substrate surface[9]

$$J_s(0, \lambda, T_s, T_{surf}) = \varepsilon_s \pi I_s(\lambda, T_s)_{BB} + \rho_s(\lambda) \sum_i G(\lambda, T_{surf})_i F_{i \to s}$$

where $\rho_s(\lambda)$ is the substrate spectral reflection coefficient, $G(\lambda)_i$ is the incident spectral irradiation on the substrate from the i-th enclosure surface at temperature T_{surf} and $F_{i \to s}$ is the radiation view factor defined below. In general not all of the radiation from the surrounding surfaces reaches the substrate surface. The fraction of emitted radiation from the surroundings that intercepts the substrate surface can be determined from a view factor or configuration factor which is a function of geometry. The view factor $F_{1 \to 2}$ is defined as the portion of radiation leaving surface S_1 and intercepting surface S_2, that is

$$F_{1 \to 2} = \frac{\text{Radiation leaving } S_1 \text{ and intercepting } S_2}{\text{Total Radiation leaving } S_1}$$

Catalogs of configuration factors are available for diverse geometries.[14]

As a simple application of a configuration factor, consider two parallel coaxial circular disks of radius r_1 and r_2 with surface areas of A_1 and A_2 separated by a centerline distance h. One disk (Fig. 9) corresponds to the anode surface and the other corresponds to the calcium fluoride window located at $h = 5$ mm above the anode surface. The configuration factor for exchange of radiant energy *from* A_1 *to* A_2 (anode to window) is denoted by $F_{1 \to 2}$ and given by [15]

$$F_{1 \to 2} = \frac{1}{2}\left(X - \sqrt{X^2 - 4\left(\frac{R_2}{R_1}\right)^2}\right) \qquad X = 1 + \frac{1 + {R_2}^2}{R_1} \qquad R_1 = \frac{r_1}{h} \quad R_2 = \frac{r_2}{h}$$

The configuration factor for exchange of radiant energy *from* A_2 *to* A_1 (window to anode) is denoted $F_{2 \to 1}$ and by the reciprocity theorem[16] is given by

$$F_{2\to1} = \frac{A_1}{A_2} F_{1\to2}$$

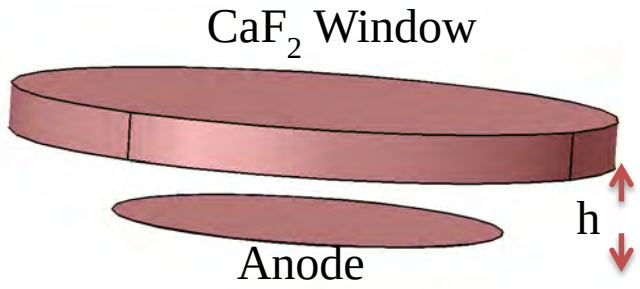

Figure 9. Anode-Window Geometry.

The calculated configuration factors for this geometry along with the spectral properties of the component materials are given in Table 1. The anode is treated as a nickel surface with an emissivity ε of 0.15 as described above. The window is treated as a grey body over the spectral range of interest.

Table I Anode-Window Configuration Factors (h =5 mm) and Surface Properties

Surface	Radius (cm)	Area (cm^2)	$F_{i\to j}$	ε(λ)	ρ(λ)	τ(λ)
Anode (1)	1.296	5.277	0.9082	0.15	0.85	0
Window (2)	2.002	12.57	0.3807	0.03	0.028	0.94

The spectral intensity emitted from the window is given by $I(\lambda, T_{win}) = \varepsilon_{win} I(\lambda, T_{win})_{BB}$ where ε_{win} is the spectral emissivity. The spectral radiosity incident on the anode surface is given by

$$G_{win}(\lambda, T_{win}) = \varepsilon_{win} \pi I(\lambda, T_{win})_{BB} F_{2\to1}$$

The emissivity of a 3 mm thick calcium fluoride window was determined from an absorption spectrum. Figure 10 shows the derived CaF_2 window emissivity. The feature near 4.26 μm (2349 cm^{-1}) is due to atmospheric interference from carbon dioxide in the spectrometer. Water vapor is also present as seen around 6.2 μm. Using the values from Table 1, and the expression

$$\frac{\varepsilon_{win} \pi I(\lambda, T_{win})_{BB} F_{2\to1} \rho_s(\lambda)}{\varepsilon_s \pi I_s(\lambda, T_s)_{BB} + \rho_s(\lambda) \varepsilon_{win} \pi I(\lambda, T_{win})_{BB} F_{2\to1}} = \frac{\varepsilon_{win} F_{2\to1} \rho_s(\lambda)}{\varepsilon_s + \rho_s(\lambda) \varepsilon_{win} F_{2\to1}}$$

for the fraction of incident spectral radiosity, one determines that the window contributes 6.1% reflected radiation to the observed signal from the anode.

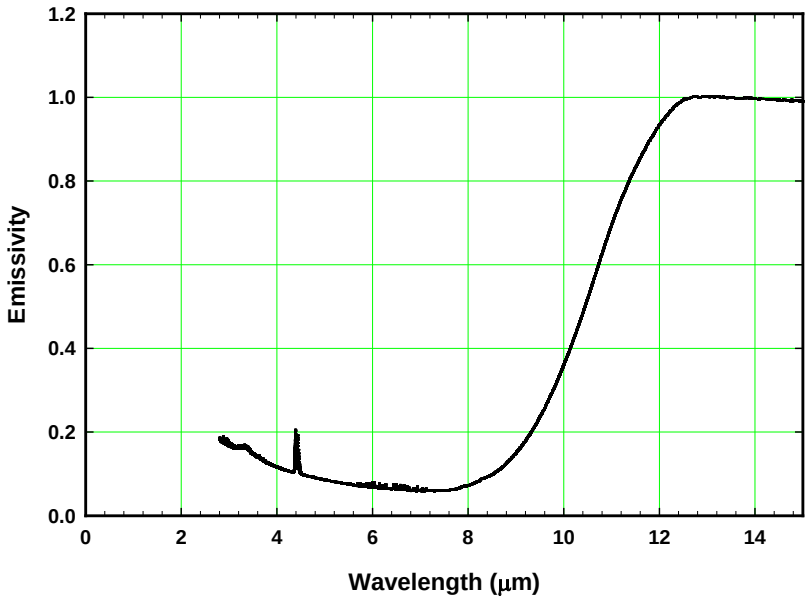

Figure 10. Emissivity of 3 mm thick CaF_2 window.

The calculation of radiation from the cylindrical side wall to the anode surface requires the numerical evaluation of the configuration factors for a cylindrical strip (wall) to a disk (anode). The geometry is shown in Figure 11. The outer strip is 5 mm in height and has a radius of 2 cm. Part of the vertical wall is hidden for clarity. The configuration factors were calculated using COMSOL's version 5.1 surface-to-surface radiation module and are given in Table 2. The wall is Al_2O_3. The emissivity of the Al_2O_3 was taken from reference 17.

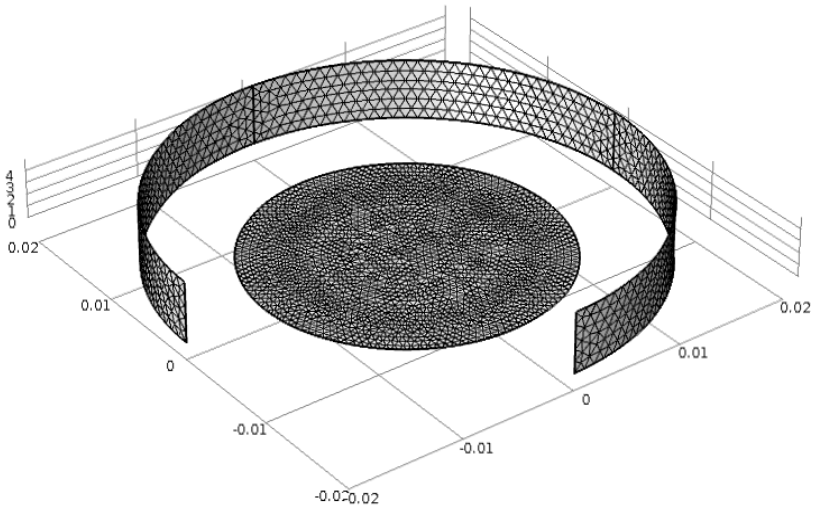

Figure 11. Side Wall to Anode geometry

Table 2 Anode-Wall Configuration factors and Surface Properties

Surface	Radius (cm)	Area (cm^2)	$F_{i\rightarrow j}$	$\varepsilon(\lambda)$	$\rho(\lambda)$	$\tau(\lambda)$
Anode (1)	1.296	5.277	.09151	.15	.85	0
Wall (2)	2.002	6.289	.07681	.40	.60	0
Wall (2→2)			.1172			

The wall to anode contribution to the signal is 14.8 % for the assumed geometry. The third configuration factor in Table 2 arises from the fact that the outer wall "sees itself" in the radiative transfer process. Note that we have utilized gray body properties for the materials, assumed a uniform spatial temperature and treated the reflecting surfaces as diffuse reflectors. As the wall's height increases, which corresponds to placing the anode deeper into the furnace tube, the wall to anode configuration factor will increase along with the background radiation. Given the spectral properties of the wall and anode, the spectral emission intensity could be calculated over a range of wavelengths using the same algorithm.

The corrections for the wall effects presented here assume that there is no participating (i.e. absorbing and emitting) gas located within the enclosure. The corrections would be applicable to surface emissivity measurements in the absence of a participating gas. The presence of a gaseous overlayer modifies the incident radiosity due to absorption and emission along the propagation path and complicates the analysis. There are several methodologies described in detail by Modest[18] for treating this type of problem. These include the Monte Carlo method, the spherical harmonic method and the discrete ordinate method. This aspect of the emission will be the subject of a future report.

CONCLUSION

An analytic model for the spectral emission intensity of a hot gas located above a substrate has been developed. The substrate contribution to the observed spectrum is nonlinear since the effective spectral emissivity $\varepsilon_{\mathrm{eff}}$ of the composite system is given by

$$\varepsilon_{\mathrm{eff}}(\lambda) = \varepsilon_{\mathrm{s}}(\lambda) + \varepsilon(\lambda, \mathrm{s})\text{-}\varepsilon_{\mathrm{s}}(\lambda)\varepsilon(\lambda, \mathrm{s})$$

where $\varepsilon_{\mathrm{s}}(\lambda)$ denotes the substrate emissivity and $\varepsilon(\lambda, \mathrm{s})$ is the spectral emissivity of the gas layer above the substrate surface. The product $\varepsilon_{\mathrm{s}}(\lambda)\varepsilon(\lambda, \mathrm{s})$ is on the order of one percent for the emissivities used in this report. Direct subtraction of the substrate background does not completely remove the substrate interaction with the gas emission spectrum. Upon linear subtraction of the background contribution, the "corrected" spectral intensity is given by

$$\mathrm{I}(\lambda, \mathrm{T_g}) = \varepsilon(\lambda, \mathrm{T_g})\mathrm{I}(\lambda, \mathrm{T_g})_{\mathrm{BB}}[1 - \varepsilon_{\mathrm{s}}(\lambda)]$$

The first two factors in this equation correspond to the selective molecular emission of the gaseous overlayer, which is linear in emitter concentration. The third factor represents the effect of the substrate emissivity and reduces the magnitude of the "corrected" spectral intensity.

The spectral emissivity of a gas can be calculated from first principles utilizing quantum mechanics and statistical mechanics[19]. In this report, we have used the HITRAN[11] data base in conjunction with the Spectral Calculator software[12] to calculate the gas emissivity of CO_2 within a spectral band centered at 2349 cm^{-1} (4.26 μm).

To illustrate the validity of the analytic model, the in-band radiance for the carbon dioxide antisymmetric stretch from 2200 cm^{-1} to 2400 cm^{-1} was calculated numerically utilizing the commercial code Spectral Calculator and compared with the analytic model prediction. The results were identical. An overview of the effects of the furnace walls on the observed emission spectrum has been presented. The analysis is very dependent upon the detailed experimental configuration and material properties such as emissivity and the nature of the emitting surface (diffuse or specular reflector). The observed spectral emission can depend upon the location of the system within the furnace since emitted wall radiation can interact with the gas and the substrate through the radiative configuration factor and can contribute to the observed spectral radiant intensity. The reflective contribution is on the order of 15 %.

The contributions from the surrounding surfaces to the spectral intensity described here do not include the effects of a participating gas layer interacting with the radiation from the configuration factor contributions. Such an analysis requires the numerical techniques described by Modest[18] and can be implemented in COMSOL. However, the analysis is applicable to corrections for surface emissivity measurements.

REFERENCES

1, Pomfret, M.B., Owrutsky, J. C., and Walker, R.A., “In Situ Studies of Fuel Oxidation in Solid Oxide Fuel Cells,” Anal. Chem. 79, 2367 (2007).

2. Pomfret, M.B., Owrutsky, J.C., and Walker, R.A. “Optical Studies of Solid Oxide Fuel Cells,” Annual Review Anal. Chem., 3, 151 (2001).

3. Kevin S. Blinn, Harry Abernathy, Xiaxi Li, Mingfei Liu, Lawrence A. Bottomley and Meilin Liu. “Raman spectroscopic monitoring of carbon deposition on hydrocarbon-fed solid oxide fuel cell anodes” Energy and Environmental Science, 5 (2012) 7913-7917.

4. E. Brightman, R. Maher, G. J. Offer, V. Duboviks, C. Heck, L. F. Cohen, and N. P. Brandon. “Designing a miniaturized heated stage for in situ optical measurements of solid oxide fuel cell electrode surfaces, and probing the oxidation of solid oxide fuel cell anodes using in situ Raman spectroscopy” Review of Scientific Instruments, 83 (2012) 053707-01 – 053707-07.

5. Michael B. Pomfret, Robert A. Walker, and Jeffrey C. Owrutsky. “High-Temperature Chemistry in Solid Oxide Fuel Cells: In Situ Optical Studies.” Journal of Physical Chemistry Letters, 3 (2012) 3053-3064.

6. M. B. Promfret, D. A. Steinhurst, & J. C. Owrutsky, “Identification of a Methane Oxidation Intermediate on Solid Oxide Fuel Cell Anode Surfaces with Fourier Transform Infrared Emission,” J. Phys. Chem. Lett. 2013, **4**, 1310-1314.

7. Y. Takahashi, Y. Shiratori, S. Furuta, K. Sasaki. "Thermo-mechanical reliability and catalytic activity of Ni–Zirconia anode supports in internal reforming SOFC running on biogas" Solid State Ionics 225 (2012) 113-117.

8. Yi Yu, Baohua Mao, Aaron Geller, Rui Chang, Karen Gaskell, Zhi Liu and Bryan W. Eichhorn, "CO2 activation and carbonate intermediates: an operando AP-XPS study of CO_2 electrolysis reactions on solid oxide electrochemical cells" Physical Chemistry Chemical Physics 16 (2014) 11633-11639.

9. J. A. LaFemina and H. D. Ladouceur, "Radiative Heat Transfer and Selective Emission in Planar Slab Coatings on Hot Emissive Substrates," NRL Memorandum Report 9073, December 31, 1987.

10. Michael F. Modest, *Radiative Heat Transfer*, 3rd ed., Academic Press, New York, 2013.

11. L.S. Rothman, I.E. Gordon, R.J. Barber, H. Dothe, R.R. Gamache, A. Goldman, V. Perevalov, S.A. Tashkun, and J. Tennyson, J. Quant. Spectroscopy and Rad. Transfer **111,** 2139-2150 (2010).

12. SpectralCalc.com, propriety software, GATS, Inc., Newport News, VA 23606, USA.

13. I. Setien-Fernandez, T. Echaniz, L. Gonzalez-Fernandez, R.B. Perez-Saez, and M. J. Tello, "Spectral emissivity of copper and nickel in the mid-infrared range between 250 and 900 °C, International Journal of Heat and Mass Transfer, 71 (2014) 549-554.

14. http://www.thermalradiation.net/indexCat.html

15. Michael F. Modest, *Radiative Heat Transfer*, 3rd ed., Academic Press, New York, 2013, page 844, Table entry 40.

16. Robert Siegel, John R. Howell, *Thermal Radiative Heat Transfer,* 2nd ed., McGraw-Hill, New York, 1981, page 187.

17. G. Teodorescu, P. D. Jones, R.A. Overfelt, and B. Guo, "Spectral-Directional Emittance of 99.99% Aluminum, Thermally Oxidized Below Its Melting Point," International Journal of Thermophysics, Vol. 27, No. 2, March 2006. See figure 2.

18. Michael F. Modest, *Radiative Heat Transfer*, 3rd ed., Academic Press, New York, 2013, pp 299-300. See Chapters 15, 16, 17, 18 and 21 for detailed discussion.

19. S. S. Penner, *Quantitative Molecular Spectroscopy and Gas Emissivities,* Addison-Wesley, Reading, MA, 1960.